JOURNAL OF SPACECRAFT AND ROCKETS
Vol. 35, No. 1, January–February 1998

Instrument for Measuring Spacecraft Potential

Luke Goembel*
Goembel Lab and Consulting, Inc., Baltimore, Maryland 21217
and
John P. Doering†
Johns Hopkins University, Baltimore, Maryland 21218

A high-resolution, low-energy electron spectrometer can be deployed on rockets or satellites to measure absolute spacecraft floating potential relative to true (Earth) ground with an accuracy of ±0.2 V. Features due to the photoionization of nitrogen and atomic oxygen by an extremely sharp solar extreme ultraviolet line (304 Å, He II) appear in the electron spectra collected by the instrument. At altitudes where the photoelectron production is local (below 250 km), the peaks that appear in the spectrum are created by electrons of a known kinetic energy: the energy of the ionizing photon minus the energy needed to ionize either atomic oxygen or molecular nitrogen. The spacecraft potential is determined from the apparent shift in the energy of the photoelectron spectral peaks. The instrument is best suited for use in the daytime atmosphere at altitudes between 150 and 250 km. The spectrometer is based on an earlier design, that of the photoelectron spectrometer of the Atmosphere Explorer satellites. Enhancements of the earlier design, including a threefold greater throughput and a specialized scan mode, greatly improve the determination of spacecraft potential. The placement of the instrument on the spacecraft is critical to the success of the measurements.

Nomenclature

D	= electrostatic (deflection) potential between the inner and outer hemispherical surfaces
D_{peak}	= electrostatic potential applied to pass electrons at the centroid of the electron spectral peak
E_{pass}	= kinetic energy of the electrons that pass through the analyzer
$E_{pass(peak)}$	= kinetic energy of the electrons passed by the spectrometer at the centroid of the electron-spectral peak
E_{source}	= kinetic energy of the electrons as produced by the source
E_λ	= the energy of the photoionizing photon
IP	= ionization potential of the atom or molecule to the final state of the ion
k	= deflection constant for the electron spectrometer
$N_2^+(A^2\Pi_u)$	= excited electronic state of singly ionized molecular nitrogen
$N_2^+(B^2\Sigma_u^+)$	= excited electronic state of singly ionized molecular nitrogen
$N_2^+(X^2\Sigma_u^+)$	= ground electronic state of singly ionized molecular nitrogen
$O^+(^2D)$	= excited electronic state of singly ionized atomic oxygen
$O^+(^2P)$	= excited electronic state of singly ionized atomic oxygen
$O^+(^4S)$	= ground electronic state of singly ionized atomic oxygen
V_{fl}	= spacecraft floating potential relative to absolute ground
$V_{instrument}$	= instrument chassis potential relative to absolute ground
V_-	= electrical potential applied to the outer hemisphere relative to instrument chassis potential
V_+	= electrical potential applied to the inner hemisphere relative to instrument chassis potential
$\Delta E/E$	= electron spectral peak width normalized for the energy location of the peak

Received Nov. 26, 1996; revision received Nov. 2, 1997; accepted for publication Nov. 10, 1997.

*President, 1413 John Street. Member AIAA.
†Professor, Department of Chemistry, Charles and 34th Streets.

Introduction

IN the ionosphere, spacecraft pass through a plasma of free electrons and positively charged ions. The electrons that strike the spacecraft supply a negative current to the spacecraft. The ions that strike the spacecraft supply a positive current. Photoemission of electrons from sunlit surfaces and the ejection of secondary electrons from surfaces impacted by energetic particles supply an additional positive current. The voltage at which all of the currents balance to zero is the floating potential of the spacecraft (the potential of the conducting surfaces that are used as the spacecraft's electrical ground measured relative to absolute, or Earth, ground). For satellites in low Earth orbit the spacecraft charges to some negative potential, usually around −1 V (Refs. 1 and 2). However, it is not yet possible to predict exactly what a spacecraft's floating potential will be under all conditions.[3]

Because charging can be a problem for spacecraft systems,[4] sounding rockets have been launched to test the effectiveness of grounding schemes.[5] Over the decades various methods have been used to determine spacecraft potential.[6–8] However, the determination of spacecraft potential with precision has proven very difficult. Multiple techniques used on a single spacecraft have yielded widely differing results.[9]

We have developed a new technique for determining spacecraft potential while analyzing old satellite data for another purpose.[10] The technique is based on the interpretation of an apparent shift in the energy location of photoelectron spectral peaks.

Spacecraft Potential from Photoelectron Spectra

Over the decades many instruments have been flown to explore the free electron energy distribution at spacecraft altitudes. Six spectrometers that flew on three satellites in the 1970s retrieved unusually high-resolution spectra. Those instruments, the photoelectron spectrometer experiment (PES) of the Atmosphere Explorer (AE) satellites,[11] retrieved thousands of spectra of the ambient electron environment of the Earth. PES was the first spectrometer with high enough energy resolution [2.5% $\Delta E/E$ full width at half-maximum (FWHM)] to reveal the features in the photoelectron spectrum due to

the photoionization of N_2 and O (the main ionospheric constituents) by 304-Å solar radiation.[12] Figure 1 is a high-resolution photoelectron spectrum acquired by many spinning passes of Atmosphere Explorer-E (AE-E) near perigee. AE-E, the last of the three AEs that carried PES, flew in a decaying elliptical orbit with perigee at 150 km and at an inclination of 19.8 deg to gather low-altitude data. Note that the spectrum shown in Fig. 1, with many data points for each peak, is not representative of the individual spectra retrieved by PES. In its finest energy sampling mode PES produced one spectrum each second with 0.5-eV gaps between energies. The improved resolution of the spectrum in Fig. 1 is the result of a data analysis technique that makes use of spectra obtained from the spinning spacecraft.

As the spacecraft spun, the potential of the PES instrument varied slightly with respect to the ionospheric plasma as a consequence of the $v \times B$ voltage induced in the spacecraft body.[13] Because the PES sensors were mounted on the outer surface of the 1.36-m-diam cylindrical AE spacecraft, the typical $v \times B$ voltage induced along the direction normal to the v and B across the conducting spacecraft body by the geomagnetic field was of the order of 0.3 V. When the spacecraft was spinning at 4 rpm, the sensor energy channels appeared to shift sinusoidally relative to the ionospheric plasma by this voltage. The magnitude of the $v \times B$ voltage was calculated for each 1-s voltage scan during the spin cycle, the center energies of the 64 channels from 0 to 34 eV were corrected by this amount, and the result was displayed as a spectrum having a greatly increased number of data points. The enhanced spectrum illustrates the full-energy resolution of the AE/PES instrument.

The absolute spectroscopic production lines dominate in the ambient photoelectron spectrum. The peaks centered at 22.2, 23.9, 25.2, and 27.2 eV are due to the electrons ejected from O and N_2 through photoionization by the extremely sharp and intense solar 304-Å line. During solar minimum the 304-Å line is an order of magnitude more intense than other photoionizing solar radiation. The lowest energy peak in Fig. 1 is due to the production of $O^+(^2P)$ and $N_2^+(B^2\Sigma_u^+)$, the second peak is due to the production of $O^+(^2D)$ and $N_2^+(A^2\Pi_u)$, the third peak is due to the production of $N_2^+(X^2\Sigma_u^+)$, and the fourth peak is due to production of $O^+(^4S)$. In addition to the four peaks that dominate the spectrum, lower-intensity echo peaks appear due to the photoionization of N_2 and O by the lower-intensity 256- and 386-Å solar radiation. Table 1 identifies each of the peaks in Fig. 1.

The two spectra in Fig. 2 are typical of those from PES. The data are from the downleg of the orbit of AE-E on Jan. 5, 1976, starting at 11:30 universal time. The energies were sampled by increasing the deflection voltage of the PES electrostatic analyzer in steps; 64 discrete electron energies (channels), evenly spaced from 0 to 34 eV, were sampled each second. The deflection voltage applied to the spectrometer for each channel was not varied over the lifetime of the instrument. For the spectra of Fig. 2, the data from 15 consecutive 1-s spectra have been accumulated to increase signal to noise enough that the four peaks due to the photoionization of N_2 and O by 304-Å solar radiation stand out. The spectra, one from 250 km and the other from 150 km, were produced by accumulating the electron counts for each of the 20 channels that correspond to the 20–30 eV portion of the 0–34 eV scanned by PES. An examination of the two spectra reveals a shift in the channels at which the spectral peaks appear. The energy scale for the plot has been adjusted so that the peaks in the spectrum from 250 km appear at the energies corresponding to those expected for the photoionization of N_2 and O. The lower-altitude spectrum exhibits an approximately one-channel shift in the location of the photoelectron peaks, corresponding to an apparent shift in the energy location of the peaks of approximately +0.5 eV. As the satellite dipped to lower altitudes, the spacecraft potential became more positive by approximately 0.5 eV, and this caused a change in the reference voltage of PES. The change in instrument potential for PES produced a change in the energy of the electrons sampled at each channel of PES. The shift in the channel location of the peaks takes place in the downleg, and then another shift

Table 1 Assignment of peaks in Fig. 1

Peak	Energy (centroid of peak), eV
368.07 Å MG IX	
$O^+(^2P)$ and $N_2^+(B^2\Sigma_u^+)$	15.1
$O^+(^2D)$ and $N_2^+(A^2\Pi_u)$	16.8
$N_2^+(X^2\Sigma_u^+)$	18.1
$O^+(^4S)$	20.1
303.78 Å HE II	
$O^+(^2P)$ and $N_2^+(B^2\Sigma_u^+)$	22.2
$O^+(^2D)$ and $N_2^+(A^2\Pi_u)$	23.9
$N_2^+(X^2\Sigma_u^+)$	25.2
$O^+(^4S)$	27.2
256.32 Å HE II	
$O^+(^2P)$ and $N_2^+(B^2\Sigma_u^+)$	29.8
$O^+(^2D)$ and $N_2^+(A^2\Pi_u)$	31.5
$N_2^+(X^2\Sigma_u^+)$	33.1
$O^+(^4S)$	34.8

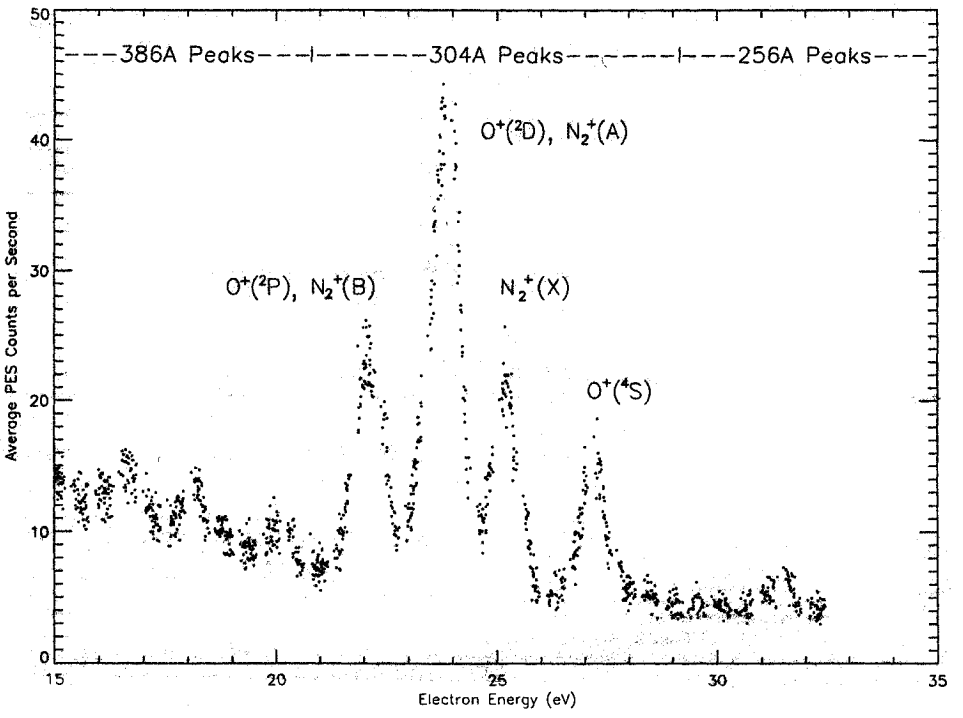

Fig. 1 High-resolution electron spectrum composed from PES data from many orbits of AE-E: improved-resolution PES data (180–205 km).

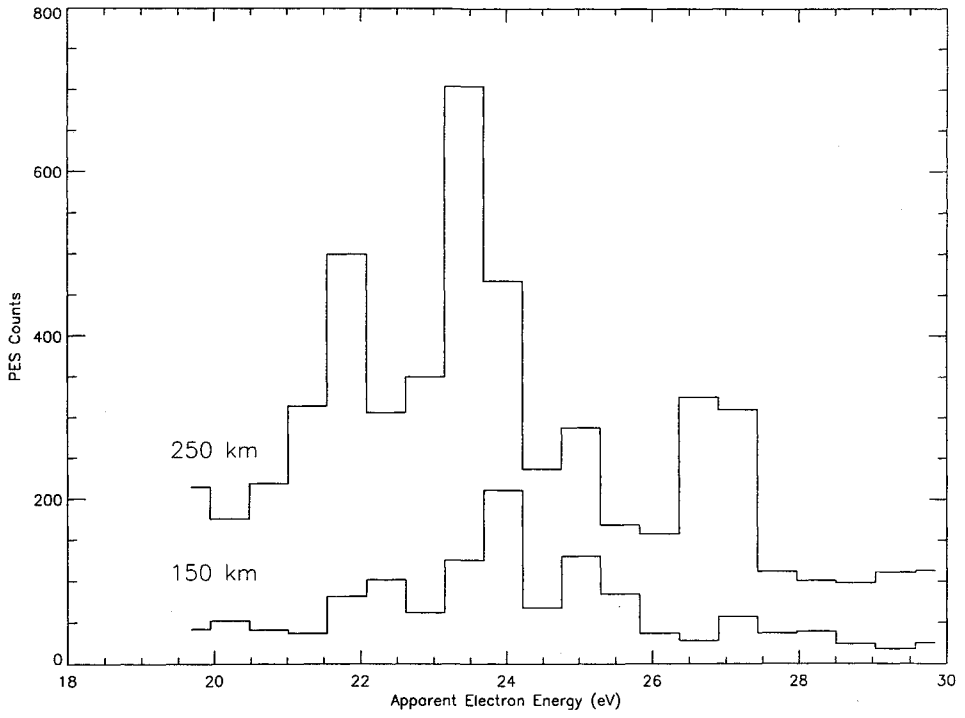

Fig. 2 Typical 15-s accumulations of PES data that illustrate the shift in spacecraft potential with altitude.

(back to the original location) takes place in the upleg for each of the orbits we have examined.[10] The cylindrical electrostatic probe[14] gives a spacecraft potential of approximately −0.9 V at 250 km and a spacecraft potential of approximately −0.5 V at 150 km for the orbit of Fig. 2. The shift of the peaks to about 0.5-eV higher energies at low altitudes is consistent with the shift of the spacecraft potential by about +0.4 V. The value we quote for the shift in the PES instrument potential is necessarily vague: PES sampling was too coarse for a more precise determination.

We believe that the phenomenon exhibited in Fig. 2 can be exploited to determine spacecraft potential in the daytime atmosphere from 150 to 250 km. At altitudes below 150 km, attenuation of the solar 304-Å flux is so great that electron counting rates would be very low and it would be take a prohibitively long time to gather a spectrum with good signal to noise. At altitudes above 250 km, the photoelectrons detected are no longer locally produced and the photoelectron lines in the spectrum may be broadened and shifted (by less than 0.5 eV) because of scattering by the ambient thermal plasma. However, the effect is variable,[15] and it may be possible to determine spacecraft potential at higher altitudes in cases where the scattering is minimal (when the thermal plasma density is low in the flux tube for the escaping photoelectrons). Although it will not be discussed further, it may also be possible to measure the spacecraft floating potential under all conditions where photoelectron spectra can be collected, with less accuracy, by examining spectra for the characteristic reduction in photoelectron fluxes that occurs at approximately 60 eV.

Physical Basis of the Measurement

The electron spectrometer described here passes electrons of energy E_{pass} with the following relationship:

$$E_{pass} = kD \tag{1}$$

where D is the deflection voltage applied. The deflection voltage is divided between the inner and outer hemispherical electrostatic surfaces so that a negative potential (relative to the instrument chassis potential) is applied to the outer hemisphere and a positive potential of approximately the same magnitude is applied to the inner hemisphere.[16–18]

Equation (1) can be applied to the case where a spectrum of a monochromatic source of electrons is collected:

$$E_{pass(peak)} = kD_{peak} \tag{2}$$

Note that $E_{pass(peak)}$ is not necessarily the kinetic energy of the electrons as produced by the source. It is possible that the electrons have been accelerated or decelerated before entering the spectrometer. Such would be the case if the instrument chassis potential were above or below true ground. The relationship between the instrument chassis potential, the kinetic energy of the electron as produced by the source, and the kinetic energy of the electron passed by the spectrometer at the centroid of the peak is

$$E_{source} = E_{pass(peak)} - V_{instrument} \tag{3}$$

If the spectrometer chassis potential is identical to the spacecraft floating potential, then

$$V_{fl} = V_{instrument} \tag{4}$$

By combining Eqs. (2–4) we find

$$V_{fl} = kD_{peak} - E_{source} \tag{5}$$

As shown by Eq. (5), the spacecraft's floating potential relative to true ground can be determined from the deflection voltage applied to pass electrons at an electron spectral peak, the deflection constant of the spectrometer, and the kinetic energy of the electrons produced by the electron source. In practice, we examine a photoelectron spectrum that is displayed as photoelectron counts vs E_{pass} to determine the spacecraft floating potential. Therefore, we use the following:

$$V_{fl} = E_{pass(peak)} - E_{source} \tag{6}$$

Prominent spectroscopic lines due to the solar 304-Å photoionization of molecular nitrogen and atomic oxygen appear in photoelectron spectra taken at altitudes from 150 to 250 km (Ref. 12). The photoionization process can be written as follows:

$$E_{source} = E_{\lambda} - IP \tag{7}$$

where E_{source} is the energy of the photoelectron ejected. The peak that appears at 27.2 eV in Fig. 1 is due to the 304-Å (E_{λ} = 40.8 eV for a 304-Å photon) photoionization of atomic oxygen to $O^+(^4S)$ (IP = 13.6 eV). Note that, although the 304-Å-produced peaks dominate in Fig. 1, lower-intensity peaks due to the solar 368- and 256-Å lines also appear. Once a line of the electron spectrum is identified, it may be used as E_{source} in Eq. (6) to determine spacecraft potential.

A discussion of the use of photoelectrons as E_{source} is in order. First, the electron source linewidth is considered. The photoelectron spectral peak width below 250 km is consistent with the PES instrument function convolved with a sharp line.[13] The actual production linewidth of the spectrum is not important in the determination of spacecraft potential because the location of the centroid of the peak is used to determine the spacecraft's floating potential. Second, accelerating or decelerating mechanisms between the electron source and the spectrometer are considered. Only an electric field between the source of the photoelectrons and the spectrometer can accelerate or decelerate the electrons. The electrons detected travel along geomagnetic field lines from their source (O and N_2 in the atmosphere) to the spectrometer. Because electric fields parallel to geomagnetic fields rarely exist in the ionosphere, there is no mechanism to accelerate or decelerate the electrons created locally by photoionization (to within the resolution of the spectrometer).[19,20] Finally, due to the conservation of energy, any regions of charge through which the electrons pass on their way to the spectrometer (such as a charge sheath that surrounds the spacecraft) will not change the kinetic energy of the electron, E_{source}.

Advanced Electron Spectrometer

Table 2 lists selected specifications for the instrument we have developed. Although the basic design of the instrument is similar to that of its forerunner, PES, the instrument is improved over PES in a number of significant ways. We have increased the throughput threefold without increasing the size or decreasing the resolution. We have reduced instrument bulk by installing a channeltron detector (very compact and light compared with the focused mesh detector used on PES) and by installing updated, more compact electronics. We have included changes to the design of the energy analyzer that should improve the electron optical performance of the spectrometer. Two large holes in the outer hemisphere of the electrostatic analyzer of PES were eliminated. The holes in the outer hemisphere were included in the PES design to 1) reduce the scattering of light within the spectrometer and 2) admit calibration radiation from a radioactive source. However, the holes in the outer hemisphere caused nonideal behavior (such as a nonlinear relationship between the voltage applied to the hemispheres and the energy of the electrons passed[12]). After PES was flown, it was found that data taken when the sun was in the instrument's field of view were not usable. Solar extreme ultraviolet (EUV) radiation produced enough photoejected electrons (an example of the photoelectric effect at work) within the instrument to severely contaminate the data.[21] We plan to orient the spectrometer so that the sun will not enter the field of view or, alternatively, discard data taken when the sun is in the field of view. We have replaced two curved slits of PES with one aperture and one straight slit. PES had a curved exit slit and a curved entrance collimating slit. On our instrument, with a 60 × 9 deg field of view, a curved collimating slit would cause noticeable attenuation at the extremes of the field of view. We believe that the elimination of the holes in the outer hemisphere will lead to, at least, an easier calibration of the instrument and the elimination of the curved slits will lead to, at least, slightly higher throughput per steradian of view.

We have taken advantage of the improvements that have been made in electronics since PES was designed more than two decades ago. The electronics available at that time limited the data rate of PES to one 64-point spectrum every second. With the electronics available today, we can easily oversample the 2.5% energy resolution of the spectrometer. Because we need only determine the shift in the location of the four peaks due to the photoionization of N_2 and O, the instrument need not devote time to the collection of data at higher or lower energies. For the determination of spacecraft potential, we will collect data from 19 to 31 eV only, an energy range that will allow an unambiguous identification of the peaks even with a few volts shift in the instrument potential. The threefold increase in throughput combined with a narrower energy range will provide the signal-to-noise ratio needed to determine peak locations (and, thus, spacecraft potential) precisely. An exact figure for the in-flight time needed to collect data for potential determination is not possible without a test flight of the spectrometer. A preliminary estimate (based on an examination of the PES data along with the consideration that the instrument will have threefold greater throughput and scan about a third the energy range) is that we will be able to determine the spacecraft potential with an accuracy of ±0.2 eV for every 5 s of flight.

Table 2 Specifications for the spectrometer

Parameter	Specification
Particles detected	Electrons
Energy range	19–31 eV
Resolution	2.5% $\Delta E/E$ FWHM
Weight	Approximately 1 kg
Size	Approximately 11 cm diam × 19 cm
Power	Less than 3 W
Data rate	256 bytes/s
Time between V_{fl} determinations	5 s (estimated)
Accuracy of V_{fl} determinations	±0.2 V (estimated)

Principle of Operation

The instrument is based on a proven design for a hemispherical electrostatic charged particle monochromator.[22] Figure 3 is a photograph of a prototype instrument, and Fig. 4 is a cutaway drawing of the prototype. The electron optical basis of the hemispherical design has been described.[18] Charged particles enter the analyzer through a circular aperture that is kept at instrument ground potential. A potential is applied to the outer hemispherical shell. (For the detection of electrons, it is a negative potential V_-.) The inner hemispherical shell is kept at potential V_+ (a positive potential for the detection of electrons). Charged particles with a greater kinetic energy than V_{pass} will be drawn to the outer hemisphere, and particles with a lesser kinetic energy than V_{pass} will be drawn to the inner hemisphere. V_+ and V_- can be supplied by a single power supply

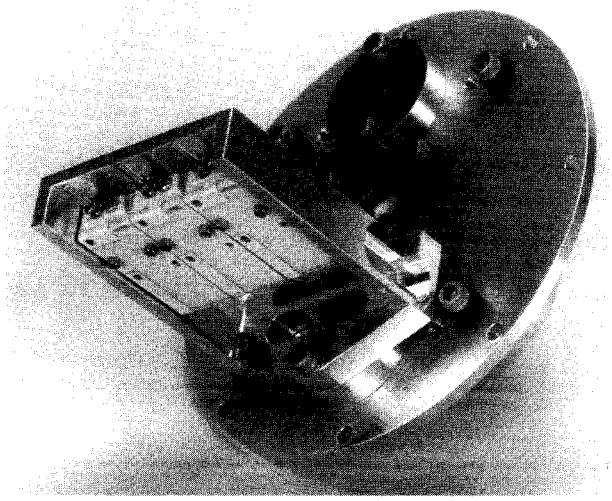

Fig. 3 Photograph of the prototype high-resolution electron spectrometer.

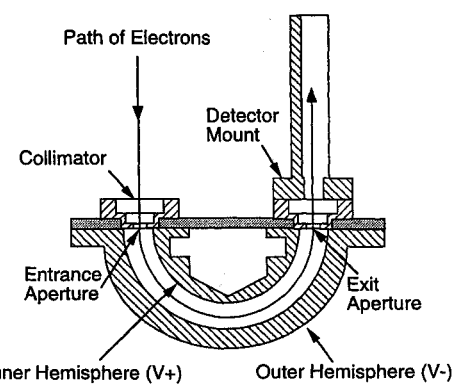

Fig. 4 Cutaway drawing of the prototype spectrometer.

if the potential is divided between the inner and outer hemispheres by a voltage divider. The relationship between V_- , V_+, and V_{pass} is well known.[18] Note that the electrostatic hemispherical analyzer discriminates by particle energy per unit charge: It cannot directly discriminate by mass. The relationship between V_-, V_+, and V_{pass} varies from instrument to instrument due to geometric differences. For example, a nonlinearity in the applied voltage vs the electron energy passed was found during the calibration of PES. As a rule, particles with a kinetic energy equal to approximately double the electrical potential provided by the power supply are passed:

$$V_{pass} \approx 2(V_+ - V_-) \tag{8}$$

Therefore, a power supply that ranges between approximately 9.5 V and approximately 15.5 V is needed to detect particles with pass energies ranging from 19 to 31 eV. The energy resolution of a hemispherical analyzer is determined by the dimensions of the slits, the inner and outer radius of the space between the hemispheres, and the field of view of the analyzer.[18]

Construction

Both the inner and outer hemispheres of the prototype spectrometer are machined from aluminum and are approximately 3 mm thick, radially. The hemispheres have been machined on a computer numerical control lathe to ±0.025-mm tolerance. The electrostatic surface of each hemisphere has been coated with an aerosol of graphite suspended in isopropyl alcohol to increase the electron sticking factor. On flight instruments we plan to machine the hemispheres to a thickness of approximately 0.5 mm to reduce the weight of the instrument while retaining (for rigidity) some thickness at the supporting base of each hemisphere. Electrostatic surfaces will be gold plated on flight instruments, rather than graphite coated, to provide a good electron sticking factor and to minimize degradation by the ambient atomic oxygen.

The insulation needed to detect particles with pass energies between 19 and 37 eV are provided by 0.25-mm-thick polyimide plastic insulators between the inner hemisphere, outer hemisphere, and ground. The collimating apertures and the focal plane apertures have been machined from 0.25-mm-thick 99% pure molybdenum sheet. The magnetic shielding for the instrument has been constructed from 80% permeability, 0.64-mm-thick mumetal. Degaussed stainless-steel machine screws have been used in the assembly of the instrument. All other parts, such as the collimator and detector mount, have been machined from aluminum.

We have chosen to use glass–ceramic channel electron multipliers. The channel electron multipliers have a large entrance aperture (10 × 5 mm) yet are compact. They are also rugged enough to withstand the rigors of launch, so that they may be used in flight versions of the spectrometer.

Positioning of Instrument on Spacecraft

The measurement of low-energy electrons in space presents a number of problems. The four major concerns are 1) the interception by the spacecraft of the particles to be measured (shadowing by the spacecraft), 2) contamination of the measurement by photoelectrons produced on sunlit parts of the spacecraft (photoemission) within the magnetic look cone of the spectrometer, 3) contamination of the measurement by direct sunlight into the field of view of the instrument, and 4) distortion of the measurements at low energies by magnetic fields. Our solution to concern 3) was covered in our discussion of the elimination of the PES light trap. Our solution to concern 4) is the enclosure of the instrument within a magnetic shield and its placement on the spacecraft far from sources of magnetic fields. Problems associated with shadowing and photoemission will be minimized by the careful placement of the spectrometer on the spacecraft, as described next.

Photoemitted electrons are those electrons that are released from spacecraft surfaces by the photoelectric effect. Interference by photoemission has been analyzed for the rocket flight of an early version of PES.[23] The effect of shadowing and photoemission on the spectra from PES of the AE satellites has also been analyzed.[21,24] Figure 5 has been produced from the data of Hays and Sharp[25] with the authors' permission. It illustrates that below approximately 5 eV the flux of photoelectrons from aluminum exposed to unattenuated sunlight greatly exceeds the flux of photoelectrons from the atmosphere. Interference from higher-energy electrons photoemitted from spacecraft surfaces must be considered as well. The photoelectric yield for aluminum, gold, and stainless steel is as high as 10% for photons of greater than 15 eV. The energy distribution of the photoemitted electrons is a function of the densities of electron states in the band structure of the material and the oscillator strengths for the various interband transitions involved. However, due to contamination effects, actual photoelectron energy distributions for various spacecraft materials show a strong deviation from the theoretical distributions predicted for clean metals.[26] For materials such as gold, aluminum, stainless steel, and graphite that have been exposed to the atmosphere, only a small portion of the electrons emitted is

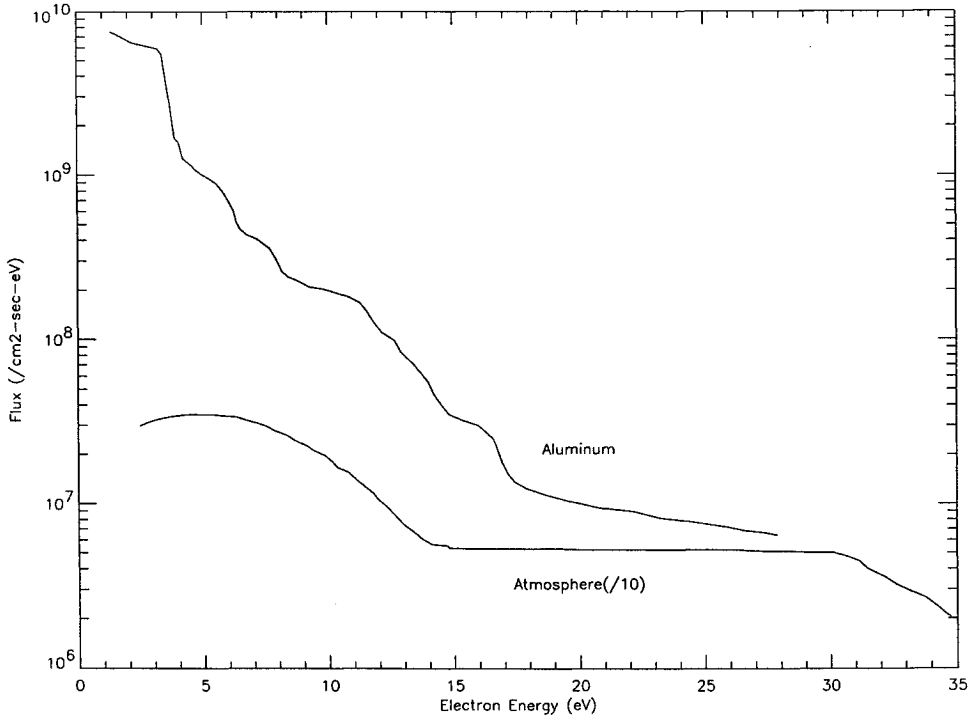

Fig. 5 Approximate photoelectron energy spectrum of aluminum and of the Earth's atmosphere (courtesy of Hays and Sharp[25]).

near the energy corresponding to the photon energy minus the work function. In the distribution of photoemitted electrons from spacecraft surfaces exposed to sunlight, a peak appears between 0 and 7 eV. The laboratory measurements of photoemission from spacecraft surfaces are consistent with the spacecraft photoemission spectrum derived from PES measurements.[24] Unfortunately, there does not appear to be a simple coating that would substantially reduce the photoemission of electrons on a spacecraft. Insulators have yields at high photon energies that exceed the yields of conductors. Of the choices between aluminum, stainless-steel, gold, insulating, or graphite-coated surfaces, graphite coating will emit the fewest photoelectrons. However, the photoyield of a graphite-coated surface still approaches that measured for metals.

One option to avoid the contamination of the spectra is to aim the spectrometer along the geomagnetic field, pointing away from the spacecraft. Electrons move along field lines with circular paths of different Larmor radii, depending on the particular energy and pitch angle. The Larmor radius (in centimeters) is approximately 5.3 times the square root of the electron energy (in electron volts). The electron may move directly up or down the field line (with a pitch angle of 180 or 0 deg), or it may move along the field line in a helical path with an intermediate pitch angle. The energy of the electron is distributed between along field-line motion and circular motion. By aiming the field of view of the spectrometer in the direction of the field line, we can minimize the admission of photoelectrons that have been produced on sunlit parts of the spacecraft. Shadowing[11] is also eliminated when the spectrometer looks along field lines.

The instrument position that is best for the particular payload is based on the orientation of the spacecraft while in flight and the locations available for placement in the payload. Consider a sounding rocket launch from the White Sands (New Mexico) Missile Range at noon on equinox, with the major axis of the cylindrical payload directed toward the sun. The geomagnetic field at White Sands is aligned at 41.5 deg from vertical (directed toward the south) at 100 km and is aligned at 41.9 deg at 300-km altitude. An ideal position for the spectrometer would be at the shaded end of the payload with the look cone centered along the magnetic field line. In that orientation, it would be impossible for an electron ejected from the surface of the spacecraft to travel into the electron spectrometer. If a position at the base of the payload were not available, however, then the instrument could be mounted to view rearward through a port cut in the cylinder wall of the payload. The look angle of the spectrometer could be oriented Earthward at an angle of 20–30 deg relative to the major axis of the payload and placed on the side of the payload that would most closely align the field of view with the geomagnetic field (Fig. 6). A detailed analysis of the paths available for electrons to reach the instrument can be made to be certain the spectra will not suffer from shadowing or from contamination[11] by electron photoemission.

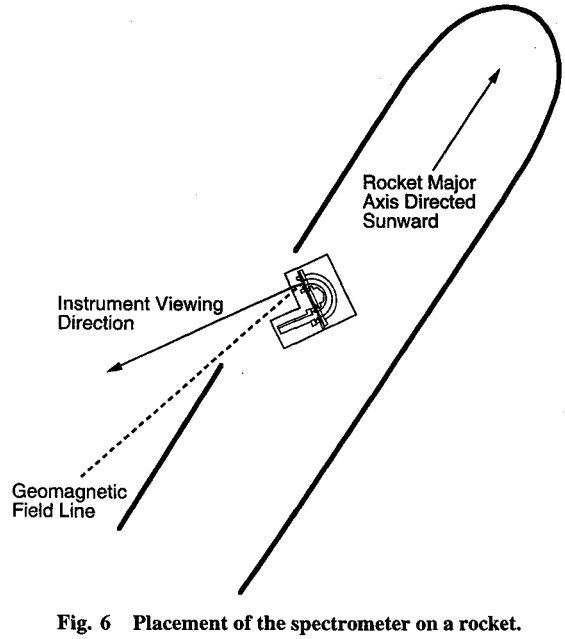

Fig. 6 Placement of the spectrometer on a rocket.

Electronics

The electronics for the spectrometer have been designed for ease of manufacture, small size, and reliability. The sensor electronics for the hemispherical analyzer consist of a channel electron multiplier, high-voltage supply, charge-sensitive preamplifier and discriminator, and line driver all in one commercially available module. The sensor electronics will mount inside the magnetic shielding. The electronics will be powered remotely from the spacecraft subsystem power supply.

The data electronics will be built around a flight-ready microprocessor, and the electronics will fit on a single, small circuit board that will be equipped with programmable memory for program storage, RAM for data manipulation and testing, and an 8-bit digital-to-analog converter for control of the analyzer potentials. A test port connector will provide an interface to a personal computer for software testing and instrument calibration.

The spectrometer will collect one full spectrum (256 bytes of data) each second to provide for good temporal resolution. The energy spectrum will range from 19 to 31 eV in 128 steps (each step will have an integration time of 7.8 ms). The count rate of the spectrometer is expected to be no higher than 39 kHz (based on the photoelectron spectra retrieved by PES on AE-E), and a 2-byte word will be sufficient to record the maximum number of counts expected at each electron energy sampled. Under conditions where electron fluxes are low (for instance, at altitudes near 150 km), successive 1-s spectra will be coadded to improve the signal to noise of the spectrum for greater certainty in the spacecraft floating potential determination.

Calibration of the Instrument

The electron energy calibration of the instrument is done within a vacuum chamber with a variable-energy electron gun.[21] The calibration consists of determining the energy of electrons admitted at each of the 128 energy channels of the instrument with the instrument chassis held at absolute (Earth) ground. The energy of the electrons from the tunable electron gun will be calibrated by use of the helium resonance phenomenon.[27] The ±0.2-eV accuracy we estimate for our spacecraft floating potential measurements is based in part on the ±0.05-eV uncertainty in the energy location of the helium resonance phenomenon. A helium cell will be placed between the electron gun and the electron spectrometer. Because the elastic scattering cross section for helium approaches zero at 19.30 eV, the helium cell will preferentially pass 19.30-eV electrons. Once the electron gun has been adjusted to produce a 19.30 ± 0.05-eV beam of electrons, adjustments can be made to produce beams of between 19.00 and 31.00 eV with a ±0.05-eV certainty in electron energy. The calibrated variable-energy gun can then be used to determine the pass energy of the spectrometer at each of the 128 deflection potentials that will be used to gather a spectrum in flight.

Additional Uses for the Spectrometer

The instrument is by no means useful only for gathering spectra for the determination of spacecraft potential. The upper bound of the detected electron energies is set by the highest potential we can supply to the hemispheres without discharge. The prototype design can scan from 1 to 4 keV with a modification of the electronics. The collection of spectra with a broader energy range than the 11 eV suggested for spacecraft potential determination would improve our understanding of the superthermal electron composition of the upper atmosphere. There are large uncertainties in the values for photoelectron fluxes provided to those who model the atmosphere. For instance, values derived from PES spectra differ by a factor of two from some of the calculated values based on solar EUV fluxes observed with optical spectrometers on the same satellite. The change in the ambient electron composition of the atmosphere with location, with season, and with changes of geomagnetic and solar activity is still not known. The data collected by the instrument could be of practical use: The quantity and energy distribution of free electrons around the Earth is of concern to those who design and operate space systems.[28–30] The development of two new uses for

high-resolution electron spectra since PES was flown [relative abundance determinations for O and N_2 (Ref. 10) and the topic of this paper, spacecraft potential determinations] multiplies the usefulness of the instrument described here for low-altitude missions, such as sounding rockets, dipping satellites, and downward-deployed tethered satellites.[31,32] The spectra returned by the instrument could be used to determine three parameters of interest: absolute photoelectron fluxes, spacecraft potential, and relative abundance of O and N_2 in the atmosphere between 150 and 250 km (Ref. 10).

Conclusion

The flight of the instrument described could provide accurate, absolute measurements of spacecraft floating potential. Although it may be possible to use the instrument to determine spacecraft potential at higher altitudes, we are confident that measurements of spacecraft floating potential can be made in the daytime atmosphere at altitudes from 150 to 250 km.

The method by which the instrument will provide spacecraft potential is based on an apparent shift in the energy location of features in high-resolution electron spectra. The shift in the energy location of peaks in the spectra is caused by the acceleration or deceleration of the electrons upon entrance of the electron spectrometer if the electron spectrometer's chassis potential differs from absolute ground. With the spectrometer chassis potential held at the spacecraft floating potential, the spacecraft floating potential can be determined from an examination of the spectra collected. To ensure that frequent measurements can be made, care must be taken in mounting the instrument so that shadowing of the photoelectrons by the spacecraft and contamination of the spectra by spacecraft photoemitted electrons may be avoided.

An estimate based on the helium cell calibration technique, past experience with laboratory measurements, and an analysis of PES spectra indicate that we will be able to determine the spacecraft floating potential to within ± 0.2 eV for every 5 s of flight. The instrument is designed to weigh less than 1 kg, occupy a volume 11 cm in diameter by 19 cm long, consume less than 3 W of power, detect electrons of between 19 and 31 eV energy, and have a data rate of 256 bytes/s.

Acknowledgments

The authors wish to thank P. G. Richards, P. T. Newell, J. O. Goldsten, and R. W. McEntire for helpful discussions during the preparation of this paper.

References

[1]Tribble, A. C., *The Space Environment: Implications for Spacecraft Design*, Princeton Univ. Press, Princeton, NJ, 1995, pp. 114, 115.

[2]Hastings, D., and Garett, H., *Spacecraft-Environment Interactions*, Cambridge Univ. Press, Cambridge, England, UK, 1996, p. 190.

[3]Cho, M., "Ionosphere Ionization Effects on Sheath Structure Around a High-Voltage Spacecraft," *Journal of Spacecraft and Rockets*, Vol. 32, No. 6, 1995, pp. 1018–1026.

[4]Shaw, R. R., Nanevicz, J. E., and Adamo, R. C., "Observations of Electrical Discharges Caused by Differential Satellite Charging," *Spacecraft Charging by Magnetospheric Plasma*, edited by A. Rosen, Vol. 47, Progress in Astronautics and Aeronautics, AIAA, New York, 1976, pp. 61–76.

[5]Pickett, J. S., Morgan, D. D., Merlino, R. L., Adrian, M. L., Berg, G. A., and Raitt, W. J., "Payload Environment and Gas Release Effects on Sounding Rocket Neutral Pressure Measurement," *Journal of Spacecraft and Rockets*, Vol. 33, No. 4, 1996, pp. 501–506.

[6]Spiegel, S. L., Saflekos, N. A., Gussenhoven, M. S., Raistrick, R. J., and Cohen, H. A., "Real-Time, Automatic Vehicle-Potential Determination from ESA Measurements: The Count-Ratio Algorithm," *Journal of Spacecraft and Rockets*, Vol. 25, No. 1, 1988, pp. 59–63.

[7]Sasaki, S., Kawashima, N., Kuriki, K., Yanagisawa, M., and Obayashi, T., "Vehicle Charging Observed in SEPAC SPACELAB-1 Experiment," *Journal of Spacecraft and Rockets*, Vol. 23, No. 2, 1986, pp. 194–199.

[8]Sasaki, S., Kawashima, N., Kuriki, K., Yanagisawa, M., Obayashi, T., Roberts, W. T., Reasoner, D. L., Williamson, P. R., Banks, P. M., Taylor, W. W. L., Akai, K., and Burch, J. L., "Neutralization of Beam-Emitting Spacecraft by Plasma Injection," *Journal of Spacecraft and Rockets*, Vol. 24, No. 3, 1987, pp. 227–231.

[9]Meyers, N. B., Raitt, W. J., White, A. B., Banks, P. M., Gilchrist, B. E., and Sasaki, S., "Vehicle Charging Effects During Electron Beam Emission from the CHARGE-2 Experiment," *Journal of Spacecraft and Rockets*, Vol. 27, No. 1, 1990, pp. 25–37.

[10]Goembel, L., Doering, J. P., Morrison, D., and Paxton, L. J., "Atmospheric O/N_2 Ratios from Photoelectron Spectra," *Journal of Geophysical Research*, Vol. 102, No. A4, 1997, pp. 7411–7420.

[11]Doering, J. P., Bostrom, C. O., and Armstrong, J. C., "The Photoelectron-Spectrometer Experiment on Atmosphere Explorer," *Radio Science*, Vol. 8, No. 4, 1973, pp. 387–392.

[12]Doering, J. P., Peterson, W. K., Bostrom, C. O., and Potemra, T. A., "High Resolution Daytime Photoelectron Energy Spectra from AE-E," *Geophysical Research Letters*, Vol. 3, No. 3, 1976, pp. 129–131.

[13]Lee, J. S., Doering, J. P., Bostrom, C. O., and Potemra, T. A., "Measurement of the Daytime Photoelectron Energy Distribution from AE-E with Improved Energy Resolution," *Geophysical Research Letters*, Vol. 5, No. 7, 1978, pp. 581–583.

[14]Brace, L. H., Theis, R. F., and Dalgarno, A., "The Cylindrical Electrostatic Probes for Atmosphere Explorer C, D and E," *Radio Science*, Vol. 8, No. 4, 1973, pp. 341–348.

[15]Lee, J. S., Doering, J. P., Potemra, T. A., and Brace, L. H., "Measurements of the Ambient Photoelectron Spectrum from Atmosphere Explorer: II. AE-E Measurements from 300 to 1000 km During Solar Minimum Conditions," *Planetary and Space Science*, Vol. 28, 1980, pp. 973–996.

[16]Kuyatt, C. E., and Simpson, J. A., "Electron Monochromator Design," *Review of Scientific Instruments*, Vol. 38, No. 1, 1967, pp. 103–111.

[17]Simpson, J. A., "High Resolution, Low Energy Electron Spectrometer," *Review of Scientific Instruments*, Vol. 35, No. 12, 1964, pp. 1698–1704.

[18]Moore, J. H., Davis, C. C., and Coplan, M. A., "Charged Particle Optics," *Building Scientific Apparatus*, 2nd ed., Addison–Wesley, New York, 1989, pp. 305–344.

[19]Peterson, W. K., and Doering, J. P., "Conjugate Photoelectron Fluxes Observed on Atmosphere Explorer C," *Geophysical Research Letters*, Vol. 4, No. 3, 1977, pp. 109–112.

[20]Peterson, W. K., Doering, J. P., Potemra, T. A., Bostrom, C. O., Brace, L. H., Heelis, R. A., and Hanson, W. B., "Measurement of Magnetic Field Aligned Potential Differences Using High Resolution Conjugate Photoelectron Energy Spectra," *Geophysical Research Letters*, Vol. 4, No. 9, 1977, pp. 373–376.

[21]Doering, J. P., Peterson, W. K., Bostrom, C. O., and Armstrong, J. C., "Measurement of Low-Energy Electrons in the Day Airglow and Day Side Auroral Zone from Atmosphere Explorer C," *Journal of Geophysical Research*, Vol. 80, No. 28, 1975, pp. 3934–3944.

[22]Goembel, L., and Doering, J. P., "A Compact, Light Weight, High Resolution Electron Monochromator," *Review of Scientific Instruments*, Vol. 66, No. 6, 1995, pp. 3472–3474.

[23]Doering, J. P., Fastie, W. G., and Feldman, P. D., "Photoelectron Excitation of N_2 in the Day Airglow," *Journal of Geophysical Research*, Vol. 75, No. 25, 1970, pp. 4787–4802.

[24]Lee, J. S., Doering, J. P., Potemra, T. A., and Brace, L. H., "Measurements of the Ambient Photoelectron Spectrum from Atmosphere Explorer: I. AE-E Measurements Below 300 km During Solar Minimum Conditions," *Planetary and Space Science*, Vol. 28, 1980, pp. 947–971.

[25]Hays, P. B., and Sharp, W. E., "Twilight Airglow 1. Photoelectrons and [OI] 5577-Angstrom Radiation," *Journal of Geophysical Research*, Vol. 78, No. 7, 1973, pp. 1153–1166.

[26]Feuerbacher, B., and Fitton, B., "Experimental Investigation of Photoemission from Satellite Surface Materials," *Journal of Applied Physics*, Vol. 43, No. 4, 1972, pp. 1563–1572.

[27]Schulz, G. J., "Experiments on Resonance in the Elastic Cross Section of Electrons on Rare-Gas Atoms," *Physical Review*, Vol. 136, No. 3A, 1964, pp. A650–A656.

[28]Vampola, A. L., "Solar Cycle Effects on Trapped Energetic Particles," *Journal of Spacecraft and Rockets*, Vol. 26, No. 6, 1989, pp. 416–427.

[29]Gorney, D. J., "Solar Cycle Effects on Near-Earth Plasmas and Space Systems," *Journal of Spacecraft and Rockets*, Vol. 26, No. 6, 1989, pp. 428–438.

[30]Walterschied, R. L., "Solar Cycle Effects on the Upper Atmosphere: Implications for Satellite Drag," *Journal of Spacecraft and Rockets*, Vol. 26, No. 6, 1989, pp. 439–444.

[31]Grassi, M., and Cosmo, M. L., "Atmospheric Research with the Small Expendable Deployer System: Preliminary Analysis," *Journal of Spacecraft and Rockets*, Vol. 33, No. 1, 1996, pp. 71–77.

[32]Anderson, J. L., "Outer Atmospheric Research Using Tethered Systems," *Journal of Spacecraft and Rockets*, Vol. 26, No. 2, 1989, pp. 66–71.

A. C. Tribble
Associate Editor